The effect of reduction potential on charge/discharge reactions on porous lead – bismuth electrodes (positives)

S. KELLY, N. A. HAMPSON

*Department of Chemistry, University of Technology, Loughborough, Leicestershire, UK*

K. PETERS

Chloride Technical Ltd, Wynne Avenue, Swinton, Manchester, UK

A series of discharge experiments were performed from the PbO_2/O_2 region to various reduction potentials using the potential step technique. Two distinct potential ranges were observed, one which occurs at potentials between 1050 and 1100 mV and the second, where there was a much larger output of capacity between 400 and 700 mV. Between these two regions there is a plateau where the relatively small output in capacity during discharge experiments enables almost complete recharging to be effected. The data presented here shows that once the electrode has entered the second reduction region it is virtually impossible to recharge the electrode using this experimental technique.

1. Introduction

The surface structure of lead electrodes in the potential range 970 to $-400\,mV^{*}$ has been studied by many workers and it is well known that the anodic corrosion films formed on lead in sulphuric acid show a multiphase structure when formed within a certain potential range [1–6]. Ruetschi [1] has reported that these corrosion films have a layer of $PbSO_4$ adjacent to the solution with an interior of tetragonal PbO and/or α-PbO_2 (PbO occurring above $-400\,mV$ and α-PbO_2 above 500 mV); these limits depend on several factors including sulphuric acid concentration, temperature and the length of the anodizing treatment. The presence of basic lead sulphates has also been reported and the most likely oxide combination is

$$PbO + \alpha\text{-}PbO_2 \qquad \text{above } 500\,mV$$

$$\alpha\text{-}PbO_2 + \beta\text{-}PbO_2 \qquad \text{above } 1100\,mV$$
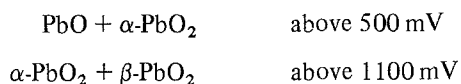
with the β-PbO_2 replacing the $PbSO_4$ at the exterior surface.

The presence of PbO in the interior of the corrosion films means that it is protected from the electrolyte by a $PbSO_4$ layer which is practi-cally impermeable to HSO_4^- and SO_4^{2-} species (once the $PbSO_4$ crystals have reached a thickness of at least $1\,\mu m$). Further corrosion then occurs by dissociation of H_2O beneath the $PbSO_4$ layer.

Pavlov and Dinev [7] looked at potential sweep experiments between -400 and 960 mV and con-cluded that the surface structure of the electrode in this region is

$$Pb/PbO \text{ layer}/PbSO_4 \text{ membrane}/H_2SO_4 \text{ solution}$$

while above 960 mV the PbO and $PbSO_4$ layers are oxidized to PbO_2. The method of oxidation (potentiostatic or galvanostatic) affects only the ratio of these phases.

Our previous work on porous lead electrodes [Pb and Pb–Sb (5%)] has shown the failure of these electrodes to accept recharge during poten-tial step cycling experiments between 700 and 1250 mV [8, 9]. We have attributed this to the formation of $PbSO_4$ crystals whose morphology is such that they resist oxidation back to PbO_2 using potentiostatic techniques. In these exper-iments the two extreme potentials were kept constant. The most positive potential (1250 mV) cannot be greatly altered; if it is made much more

---

positive, the electrode gradually becomes obscured with bubbles of oxygen. If the oxidation potential is greatly reduced then the product PbO_2 is not produced. The reduction potential can, however, be significantly altered and the effect of varying the potential on the morphology of the $PbSO_4$ crystals can be followed by noting the changes in capacity of the electrode during subsequent recharge experiments. (In general, the larger the $PbSO_4$ crystals the more resistant they will be to oxidation and the lower the recharge capacity during potentiostatic step experiments back into the PbO_2 region.)

This paper records such a series of experiments performed on a Pb–Bi binary electrode; the level of Bi chosen was 0.13% since we have previously shown it to be the most useful concentration in the practical automotive battery range [10].

2. Experimental procedure

The experimental set-up, electrode preparation and cell construction have all been fully described in previous publications [8, 9]. Chemical analysis of the alloy material used showed: 0.127% Bi, 0.0025% Ag; 0.0026% Cu and 0.0025% Ti. The porous electrode was made with a standard automotive positive paste (density $4.10 \, g \, cm^{-3}$) whose composition consisted of:

    1080 kg grey oxide (60% PbO);

    0.9 kg silica;

    78 dm^3 1.4 s.g. H_2SO_4;

    138 dm^3 H_2O.

Table 1. Discharge capacities for a series of potential-step experiments from 1250 mV on a porous Pb–Bi (0.15%) electrode in $5M \, H_2SO_4$ at $23°C$ (nominal surface area = $0.071 \, cm^2$)

Reduction potential (mV)	Total discharge capacity (C)	Time to reach total discharge (min)
1200	Zero	—
1100	10.9	92
1050	27.3	106
1000	32.1	63
950	34.7	68
700	37.7	30
400	122.0	47
20	135.6	40
− 223	151.6	50

A series of cycling experiments was performed in which a fully charged porous electrode, potentiostated at 1250 mV, was subjected to various reduction potentials using the potential-step technique. The changes in capacity with time were followed during the discharge experiment together with the variations in the current–time transient. Once the electrode was fully discharged (capacity remained constant) the corresponding oxidation pulse was carried-out back to 1250 mV (PbO_2/O_2 region). Between each charge/discharge cycle, for a certain reduction potential, the electrode was removed from the cell and oxidized galvanostatically ($\sim 25 \, mA \, cm^{-2}$) in $0.3M \, H_2SO_4$ for 3 days with oxygen being freely evolved from the electrode. This was performed with the working electrode in an upwards facing position to prevent oxygen bubbles from saturating the porous matrix. The reduction potentials reported here are 1200, 1100, 1050, 1000, 950, 700, 400, 20 and − 223 mV.
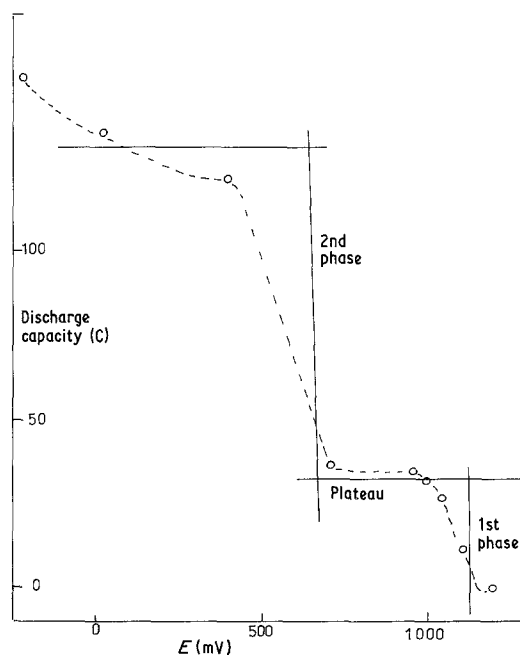

Fig. 1. Curve showing the relationship between discharge capacity and reduction potential for a series of potential-step experiments in Pb–Bi (0.13%) from 1250 mV to certain potentials in the $PbSO_4$ region ($23°$ C, $\phi = 0.071$ cm^2, $5M \, H_2SO_4$).
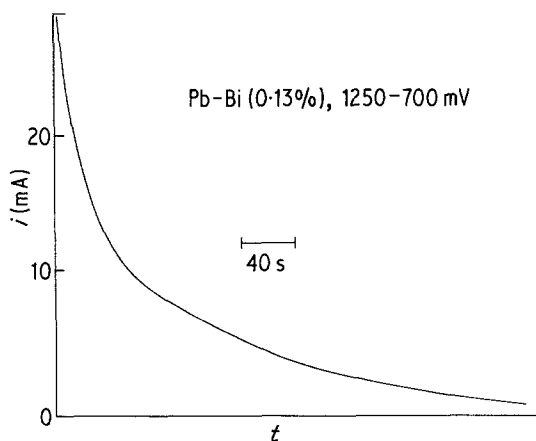
Fig. 2. Current–time transient for a potential-step experiment from 1250 to 700 mV on a Pb–Bi (0.13%) electrode at 23° C in 5 M H_2SO_4 ($\phi = 0.071$ cm²) following galvanostatic oxidation (0.3 M H_2SO_4, 25 mA cm⁻² for 3 days).

3. Results and discussion

3.1. Discharge experiments

Table 1 summarizes the total discharge capacity ($PbO_2 \rightarrow PbSO_4$) for a series of potential-sweep experiments from 1250 mV to various potentials in the range $-$ 200 to 1200 mV and the time taken for these reactions to occur. The relationship between discharge capacity and reduction potential is interesting (Fig. 1); there appears to be two distinct phases of PbO_2 reduction within the porous matrix. The first species starts to be reduced at about 1100 mV with the capacity reaching a limit at approximately 1050 mV. At about 700 mV a second species starts to be

Table 2. The current–time relationship for a series of discharge experiments to various potentials on a Pb–Bi (0.15%) electrode at 23° C in 5M H_2SO_4 ($\phi = 0.071$ cm²)

Reduction potential (mV)	Relationship
1150	$i \propto t^{-1.5}$
1000	$i \propto t^{-3.5}$
700	$i \propto t^{-4.0}$
400	$i \propto t^{-1.3}$
20	$i \propto t^{-1.7}$
$-$ 223	$i \propto t^{-1.8}$

reduced with a three-fold increase in capacity output above that of the first species. It is interesting to note that the useful lead–acid battery potential range lies on the plateau between these two phases; this may explain why successful recharge can be carried out with a lead–acid battery positive plate (where the final reduction potential lies only 300 mV below the initial starting potential and lies on the plateau shown in Fig. 1) but not with the positive electrodes in our previous experiments (where the reduction potential was 550 mV below the initial potential and lies well within the second reduction phase).

It seems likely that the initial reduction reaction is predominantly β-$PbO_2 \rightarrow PbSO_4$, although a certain amount of α-PbO_2 is also present at these potentials ($>$ 1100 mV). An explanation for the second reduction phase is rather more difficult; it is feasible that it is mainly the reduction of α-PbO_2 to form lead sulphate. The $PbSO_4$ crystals so produced are much larger than normal which accounts for the 3-fold increase in output. It seems likely, however, that the situation is more complex than
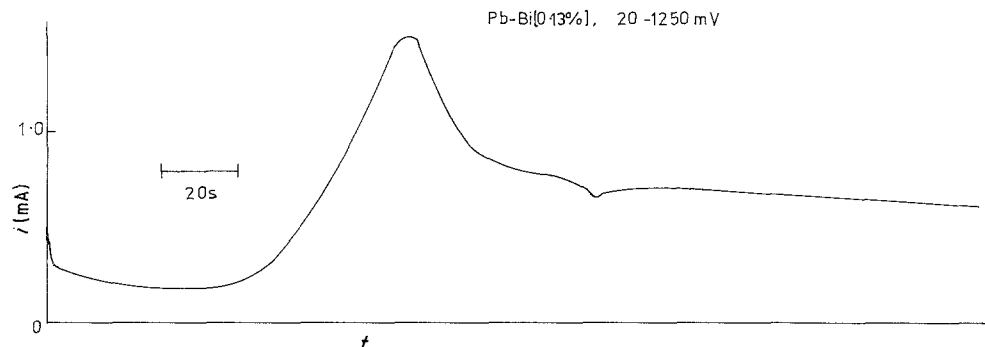

Fig. 3. Current–time transient for a potential-step experiment from 20 to 1250 mV on Pb–Bi (0.13%) following a potential-step reduction from 1250 to 20 mV. Details as for Fig. 2.
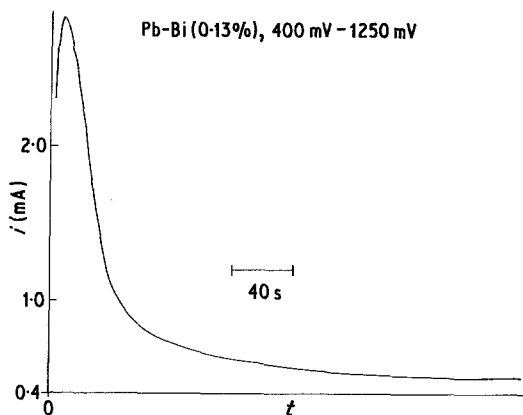
Fig. 4. Current–time transient for a potential-step experiment from 400 to 1250 mV on Pb–Bi (0.13%) following a potential-step reduction from 1250 to 400 mV.

Fig. 6. Current–time transient for a potential-step experiment from — 233 to 1250 mV on Pb–Bi (0.13%) following a potential-step reduction from 1250 to — 223 mV.

a simple fall in the current was observed. The value of the exponent did vary, however, and the data is summarized in Table 2. A large increase in the slope of the current–time curves is obtained when the reduction potential lies within one of the reduction phases shown in Fig. 1 (700 to 1000 mV).

3.2. Recharge experiments

Figs 3–6 show the current–time transients for a series of potentiostatic oxidation experiments from various reduction potentials to a set potential in the lead dioxide region (1250 mV). In each of these cases, the initial double layer charging spike is followed by an increase in the current flow; this can be attributed to the formation and growth of nucleation centres for the production of lead dioxide. The subsequent overlap of these centres results in a decrease in the current flow, the resultant pattern obtained is that of a current peak. The shape of these peaks can be seen to vary with reduction potential suggesting the formation of various types of crystal morphology. At reduction potentials greater than 700 mV, no current peak was observed during the recharge experiment (see e.g. Fig. 7) which suggests that sufficient nuclei are already present in the matrix to allow the formation of lead dioxide. We can conclude from this observation that once the second phase of reduction is entered (i.e. the final reduction potential below about 800 mV) the annihilation of nucleation centres for PbO_2 formation occurs and we observe a peak in the current–time oxidation transient.

The ability of porous Pb–Bi electrodes to accept recharge varies with reduction potential and the trend is in good agreement with our explanation of the data presented in Fig. 1. The electrode subjected to a reduction potential of

this, especially if the presence of tetragonal PbO in the matrix is also considered. The most exciting observation from these experiments is that comparatively little reduction occurs in the potential range 750 to 950 mV, enabling recharge back to PbO_2 to be carried out successfully.

Fig. 2 shows a typical current–time transient for a potential-sweep discharge experiment on a porous Pb–Bi electrode. The initial current spike can be attributed mainly to the charging of the double layer at the electrolyte–electrode interface. The absence of any further increase in the current flow indicates that sufficient nuclei are present in the porous matrix to allow the formation of lead sulphate from lead dioxide. The shape of this transient did not vary with reduction potential,
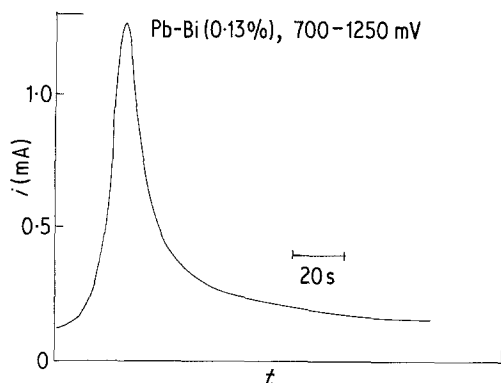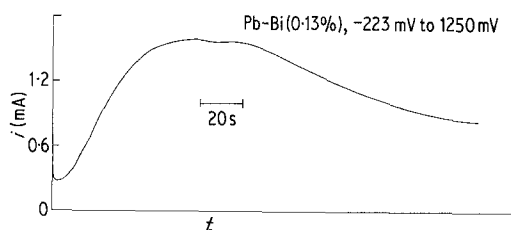

Fig. 5. Current–time transient for a potential-step experiment from 700 to 1250 mV on Pb–Bi (0.13%) following a potential-step reduction from 1250 to 700 mV.
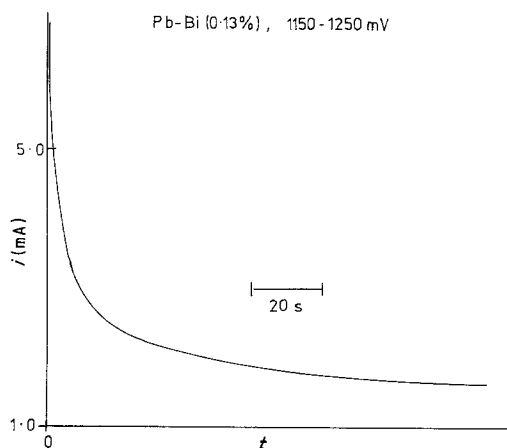
Fig. 7. Current–time transient for a potential-step experiment from 1150 to 1250 mV on Pb–Bi (0.13%) following a potential-step reduction from 1250 to 1150 mV.

950 mV (i.e. a potential on the plateau between the two reduction phases) exhibits a readiness to accept recharge during the corresponding oxidation pulse with over 88% of the total discharge capacity being accepted after only 3 h of oxidation. However, when the electrode is subjected to a final discharge potential which lies within the second reduction phase (e.g. 700 mV) the ability to accept recharge is substantially reduced (only 65% of the total discharge capacity after 3 h of oxidation).

Acknowledgement

References

[1]   P. Ruetschi, *J. Electrochem. Soc.* **120** (1973) 3, 331.
[2]   J. J. Lander, *ibid.* **98** (1951) 213.
[3]   *Idem, ibid.* **103** (1956) 1.
[4]   J. Burbank, *ibid.* **103** (1956) 87.
[5]   P. Ruetschi and R. T. Angstadt, *ibid.* **111** (1964) 1323.
[6]   E. Sato and T. Shiina, *J. Electrochem. Soc. Japan* **32** (1964) 148.
[7]   D. Pavlov and Z. Dinev, *J. Electrochem. Soc.* **127** (1980) 4, 855.
[8]   S. Kelly, N. A. Hampson and K. Peters, *J. Appl. Electrochem.* **11** (1981) 601.
[9]   *Idem, ibid.* **11** (1981) 269.
[10] *Idem, J. Electrochem. Soc.* **127** (1980) 1456.